DOI: 10.1002/ejic.200600964

# *N*-(Aryl)picolinamide Complexes of Ruthenium: Usual Coordination and Strategic Cyclometalation

**Sumon Nag,[a] Ray J. Butcher,[b] and Samaresh Bhattacharya*[a]**

**Keywords:** Picolinamide ligands / Ruthenium complexes / Cyclometalation

Reaction of five *N*-(4-*R*-phenyl)picolinamides (R = $OCH_3$, $CH_3$, H, Cl, and $NO_2$) with $[Ru(PPh_3)_2(CO)_2Cl_2]$ in refluxing 2-methoxyethanol in the presence of a base ($NEt_3$) affords two geometrical isomers of a group of complexes (**1-R** and **2-R**), each of which contains an amide ligand coordinated to the metal center as a monoanionic bidentate *N*,*N* donor along with two triphenylphosphanes, a carbonyl, and a hydride. Similar reaction of *N*-(naphthyl)picolinamide with $[Ru(PPh_3)_2(CO)_2Cl_2]$ affords an organometallic complex, **3**, in which the amide ligand is coordinated to the metal center, by C–H activation of the naphthyl ring at the 8-position, as a dianionic tridentate *N*,*N*,*C* donor along with two triphenylphosphanes and one carbonyl. Structures of the **1-$OCH_3$**, **2-$CH_3$**, and **3** complexes have been determined by X-ray crystallography. In all the complexes the two triphenylphosphanes are *trans*. In the **1-R** complexes the hydride is *trans* to the pyridine nitrogen and in the **2-R** complexes it is *trans* to the amide-nitrogen. All the complexes are diamagnetic, and show characteristic $^1H$ NMR signals and intense MLCT transitions in the visible region. Cyclic voltammetry on all the complexes shows a $Ru^{II}$–$Ru^{III}$ oxidation within 0.71–0.93 V versus SCE. An oxidation and a reduction of the coordinated amide ligand are also observed within 1.29–1.69 V versus SCE and –1.02 to –1.21 V versus SCE respectively.

(© Wiley-VCH Verlag GmbH & Co. KGaA, 69451 Weinheim, Germany, 2007)

## Introduction

There has been considerable current interest in the chemistry of ruthenium complexes, largely because of their fascinating redox, photophysical, and photochemical properties.[1] As all these properties are directed primarily by the coordination environment around the metal center, complexation of ruthenium by ligands of selected types is of significant importance. In the present study, which has originated from our continued interest in the chemistry of ruthenium in different coordination environments,[2] we have selected a group of amide ligands (**$L^1$**) derived from picolinic acid and anilines with five different *para*-substituents in order to study their influence, if any, on the redox properties of the resulting ruthenium complexes.

Chemistry of the amide ligands is of particular interest with reference to their role in biological processes.[3] For example, the amide linkage plays a key role in the formation and maintenance of protein architectures, which are crucial for their performance in biological systems.[4] The selected amide ligands (**$L^1$**) are known to bind to metal ions either as neutral *N*,*O* donors (amide form, **I**) or as monoanionic *N*,*N* donors (amidate form, **II**) by loss of the amide pro-

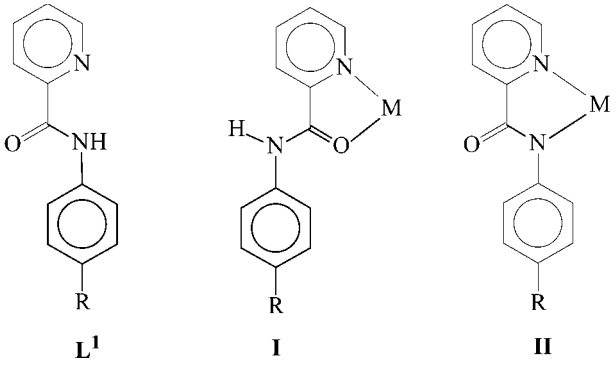


**$L^1$** **I** **II**

R = $OCH_3$, $CH_3$, H, Cl, $NO_2$

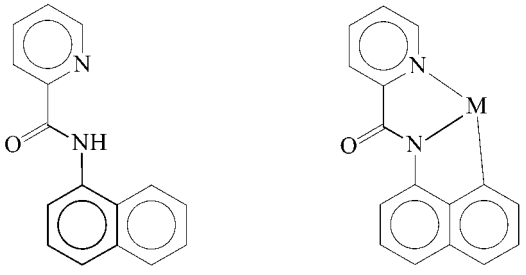


**$L^2$** **III**

[a] Department of Chemistry, Inorganic Chemistry Section, Jadavpur University,
Kolkata 700032, India
[b] Department of Chemistry, Howard University,
Washington, DC 20059, USA

Supporting information for this article is available on the WWW under http://www.eurjic.org or from the author.

 © 2007 Wiley-VCH Verlag GmbH & Co. KGaA, Weinheim 

ton.[5] Chelation in the amidate mode is known to stabilize metal ions in their high oxidation states, while that in the amide mode is reported to favor relatively lower oxidation states of a metal.[5] Interconversion between the amide (**I**) and amidate (**II**) modes of binding has been utilized to chemically manipulate redox properties of the metal center.[6] It may be mentioned here that though the chemistry of amide complexes of many transition metals has been extensively studied,[7] that of ruthenium appears to have received much less attention.[2j,8] As the source of ruthenium we have selected the $[Ru(PPh_3)_2(CO)_2Cl_2]$ complex, because of its demonstrated ability to accommodate bidentate ligands through displacement of carbonyl and chloride.[2f,2m] Reaction of the selected amides ($\mathbf{L^1}$) as well as a related ligand, viz. *N*-(naphthyl)picolinamide ($\mathbf{L^2}$), with $[Ru(PPh_3)_2(CO)_2Cl_2]$ has been found to afford interesting complexes where the amides ($\mathbf{L^1}$ and $\mathbf{L^2}$) are bound to ruthenium, as in **II** and **III** respectively. An account of the chemistry of all these complexes is presented in this report, with special reference to their formation, characterization, and spectral and electrochemical properties.

## Results and Discussion

Reactions of the *N*-(4-*R*-phenyl)picolinamides ($\mathbf{L^1}$) with $[Ru(PPh_3)_2(CO)_2Cl_2]$ proceed smoothly in refluxing 2-methoxyethanol in the presence of triethylamine. From each of these reactions two complexes were obtained, viz. a golden yellow complex and a yellow complex (**1-R** and **2-R**). The combined yield of these two complexes was reasonable.

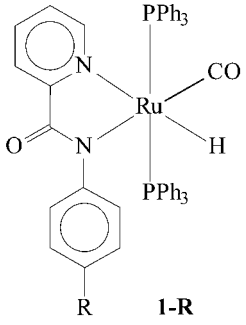


**1-R**

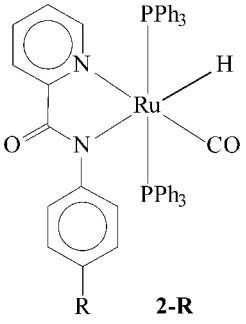


**2-R**

R = $OCH_3$, $CH_3$, H, Cl, $NO_2$

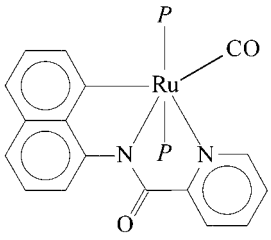


*P* = $PPh_3$

**3**

Preliminary (microanalytical, spectroscopic, magnetic, etc.) characterizations on these complexes (vide infra) indicate the presence of an amide ligand, two triphenylphosphanes, a carbonyl, and a hydride in the coordination sphere. In order to find the stereochemistries of these complexes as well as the coordination mode of the *N*-(4-*R*-phenyl)picolinamides in them, the structure of one representative complex from each family, viz. **1-$OCH_3$** and **2-$CH_3$**, has been determined by X-ray crystallography. The structure of the **1-$OCH_3$** is shown in Figure 1 and selected bond parameters are listed in Table 1.

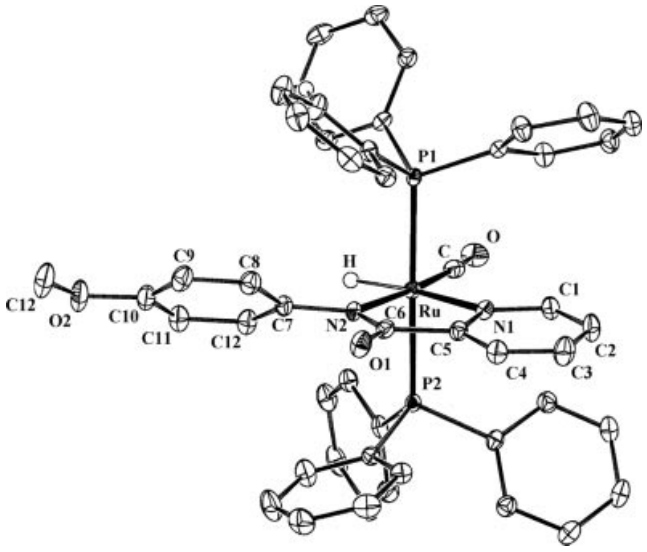


Figure 1. View of the **1-$OCH_3$** complex.

The structure shows that the *N*-(4-methoxyphenyl)picolinamide is coordinated to ruthenium, by dissociation of the acidic proton, as a monoanionic *N*,*N* donor (**II**). Two triphenylphosphanes, a hydride, and a carbonyl are also coordinated to the metal center. Ruthenium is therefore sitting in a $C_1H_1N_2P_2$ coordination environment, which is distorted octahedral in nature, as reflected in all the bond parameters around ruthenium. The coordinated picolinamide, hydride, and carbonyl constitute one equatorial plane with the metal at the center, where the hydride is *trans* to the pyridine nitrogen and the carbonyl is *trans* to the amide-nitrogen. The $PPh_3$ ligands occupy the remaining two axial positions and hence they are mutually *trans*. The observed Ru–P, Ru–C, and Ru–H distances are all quite normal,[9] and so are the bond lengths in the Ru(amide) fragment.[8b,8c] In the crystal lattice of the **1-$OCH_3$** complex, there are two water molecules present per molecule of the complex. In order to find out the link between these water molecules and the complex molecule, the packing pattern in the lattice has been scrutinized (Figure 2), which shows that a layer of water molecules lies in between two layers of complex molecules and thereby holds them together. A closer inspection into the network reveals that the methoxy-oxygen in each complex molecule is hydrogen-bonded to a phenyl hydrogen of a coordinated $PPh_3$ of an adjacent complex molecule and two such hydrogen bonds result in the formation of a dimeric unit. Four water molecules, which are interlinked by hydrogen bonds, bridge two such dimeric units by hydrogen bond formation involving the amide oxygen and a phenyl hydrogen of a $PPh_3$. These hydrogen-

 © 2007 Wiley-VCH Verlag GmbH & Co. KGaA, Weinheim 

Table 1. Selected bond lengths and bond angles for **1-OCH$_3$**, **2-CH$_3$**, and **3**.

| | | | |
|---|---|---|---|
| **1-OCH$_3$** | | | |
| Bond lengths [Å] | | | |
| Ru–C | 1.839(2) | C–O | 1.164(2) |
| Ru–N(2) | 2.1567(16) | N(2)–C(6) | 1.329(3) |
| Ru–N(1) | 2.1792(17) | C(5)–N(1) | 1.358(2) |
| Ru–H | 1.5475 | C(6)–O(1) | 1.253(2) |
| Ru–P(1) | 2.3636(5) | | |
| Ru–P(2) | 2.3689(5) | | |
| Bond angles [°] | | | |
| P(1)–Ru–P(2) | 178.495(17) | N(2)–Ru–N(1) | 76.50(6) |
| C–Ru–N(2) | 173.76(8) | Ru–C–O | 173.63(19) |
| N(1)–Ru–H | 168.3 | | |
| **2-CH$_3$** | | | |
| Bond lengths [Å] | | | |
| Ru–C | 1.844(3) | C–O | 1.162(3) |
| Ru–N(2) | 2.203(2) | N(2)–C(7) | 1.334(3) |
| Ru–N(1) | 2.152(2) | C(6)–N(1) | 1.352(3) |
| Ru–H | 1.58(3) | C(7)–O(1) | 1.249(3) |
| Ru–P(1) | 2.3687(7) | | |
| Ru–P(2) | 2.3569(7) | | |
| Bond angles [°] | | | |
| P(1)–Ru–P(2) | 172.61(2) | N(2)–Ru–N(1) | 75.46(8) |
| C–Ru–N(1) | 175.20(9) | Ru–C–O | 175.1(2) |
| N(2)–Ru–H | 170.2(9) | | |
| **3** | | | |
| Bond lengths [Å] | | | |
| Ru–C | 1.853(2) | C–O | 1.157(3) |
| Ru–N(1) | 2.1588(13) | N(2)–C(6) | 1.340(2) |
| Ru–N(2) | 2.0882(18) | C(5)–N(1) | 1.351(2) |
| Ru–C(15) | 2.0883(16) | C(6)–O(1) | 1.238(2) |
| Ru–P(1) | 2.3691(5) | | |
| Ru–P(2) | 2.3825(5) | | |
| Bond angles [°] | | | |
| P(1)–Ru–P(2) | 174.40(2) | N(1)–Ru–N(2) | 76.97(5) |
| N(2)–Ru–C | 176.48(8) | N(2)–Ru–C(15) | 80.31(6) |
| N(1)–Ru–C(15) | 157.04(6) | Ru–C–O | 176.57(17) |

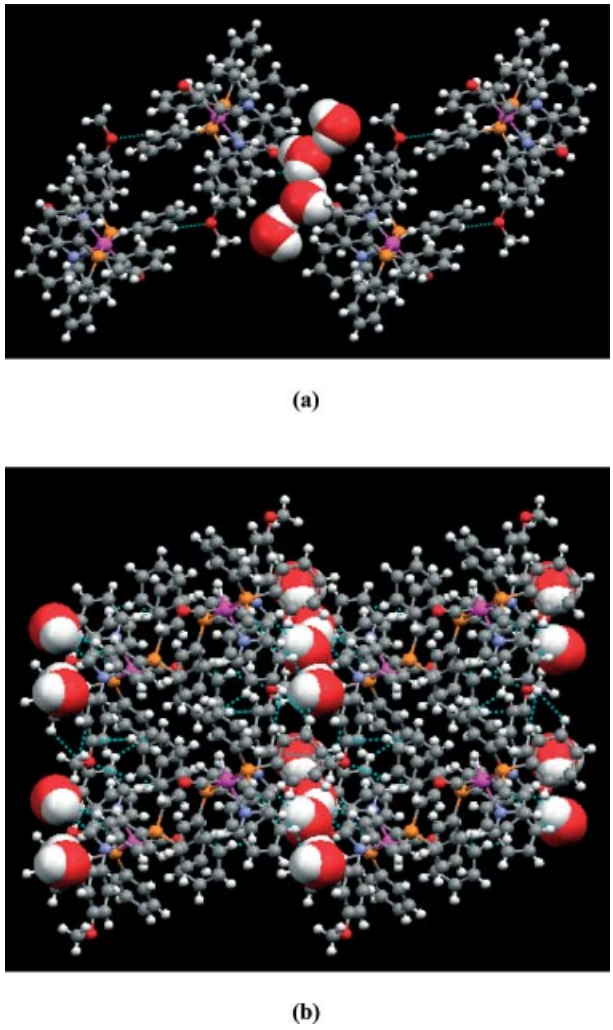


Figure 2. (a) Hydrogen bonding and (b) packing diagram (down the *b* axis) of the **1-OCH$_3$** complex.

bonding interactions in the crystal lattice appear to contribute a lot to its stability. As all the **1-R** complexes have been synthesized similarly and they show similar properties (vide infra), the other four **1-R** (R ≠ $OCH_3$) complexes are assumed to have a similar structure to the **1-OCH$_3$** complex.

The structure of the **2-CH$_3$** complex (Figure 3) shows that it is very similar to the **1-OCH$_3$** complex; the only differences are in the disposition of coordinated carbonyl and hydride with respect to the coordinated picolinamide. The hydride is *trans* to the amide-nitrogen and the carbonyl is *trans* to the pyridine nitrogen. All the bond parameters in this **2-CH$_3$** complex compare well with those observed in the **1-OCH$_3$** complex (Table 1). In the crystal lattice of **2-CH$_3$** there is one molecule of methanol per molecule of the complex. The packing pattern in the lattice shows (Figure S1, supporting information) that this methanol molecule is involved in three hydrogen-bonding interactions, two with the amide oxygen and a phenyl hydrogen of a $PPh_3$ of one

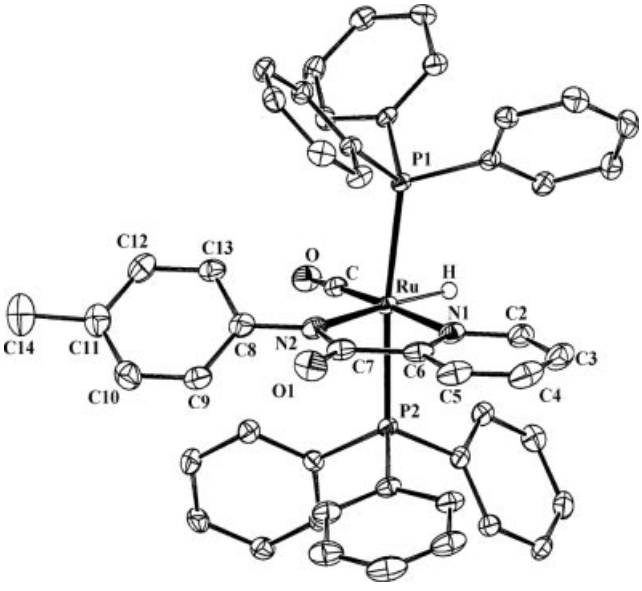


Figure 3. View of the **2-CH$_3$** complex.

 © 2007 Wiley-VCH Verlag GmbH & Co. KGaA, Weinheim 

complex molecule, and the third with the phenyl hydrogen of a $PPh_3$ of a second complex molecule. The methanol molecules thus bridge the individual complex molecules through hydrogen bonding. Based on the similarity in their synthesis and properties (vide infra), the other four **2-R** (R $\neq$ $CH_3$) complexes are assumed to have similar structures to **2-CH$_3$**. Each **2-R** complex is therefore a geometrical isomer of the corresponding **1-R** complex. The observed elemental (C, H, N) analytical data of the **1-R** and **2-R** complexes agree well with their compositions.

Formation of the two stereoisomers (**1-R** and **2-R**) from the same reaction may be rationalized in terms of Scheme 1. Upon reaction with $[Ru(PPh_3)_2(CO)_2Cl_2]$ the amide ligands (**L$^1$**) bind to the metal center, through dissociation of the acidic N-H proton, as monoanionic *N*,*N* donors with simultaneous dissociation of a CO and a chloride from the ruthenium starting complex to generate two stereoisomers (**A** and **B**) of an intermediate. These two stereoisomers, which are believed to remain in equilibrium, are probably formed by different kinetic routes. The Ru–Cl bond in these intermediates is then converted into a Ru–H bond under the prevailing reaction condition affording the **1-R** and **2-R** complexes respectively. Such conversion of a Ru–Cl bond into a Ru–H bond in alcoholic solvent in the presence of base is well documented in the literature.[10]

Disposition of the Ru–H bond with respect to the pendent phenyl ring in **1-R** points to the possibility of a C–H activation of the aryl ring. Such an activation could not take place in the **1-R** complexes, because in them the phenyl ring is not close enough to the metal center, and had the phenyl ring undergone an orthometalation it would have resulted in the formation of a sterically unstable four-membered metallacycle. In order to undergo C–H activation the aryl fragment should be so chosen that one of its C–H bonds should come in close proximity to the Ru–H bond. With this simple strategy in mind, *N*-(naphthyl)picolinamide (**L$^2$**) has been chosen as the target ligand for the C–H activation. Reaction of *N*-(naphthyl)picolinamide with $[Ru(PPh_3)_2(CO)_2Cl_2]$ has been carried out similarly as before, which has afforded an orange complex (**3**) in good yield. Preliminary characterizations on this complex indicate the presence of an amide ligand, two triphenylphosphanes, and a carbonyl in the coordination sphere, as well as the absence of any hydride. The identity of complex **3** has been revealed by its structure determination by X-ray crystallography. The structure (Figure 4) shows that *N*-(naphthyl)picolinamide is indeed coordinated to ruthenium in the expected *N*,*N*,*C* fashion (**III**). The Ru–C(naphthyl) bond is found to be normal[2m] and the other bond parameters compare well with those observed in the earlier structures (Table 1). The absence of any solvent of crystallization in the crystal lattice of complex **3** indicates the possible existence of some noncovalent interaction(s) between the individual complex molecules. A careful inspection of the packing pattern in the lattice shows that noncovalent interactions of two different types, viz. C–H···O and C–H···π interactions, are active in the lattice (Figure S2, Supporting Information). Two phenyl protons of two $PPh_3$ ligands belonging to two adjacent complex molecules are found to be hydrogen bonded to the π-cloud of two other phenyl rings of the same two $PPh_3$ ligands. However, this hydrogen-bonding interaction is directed to an edge of the phenyl ring in an $\eta^2$ fashion. The amide oxygen of a third complex molecule is also hydrogen-bonded to two phenyl hydrogen atoms of two $PPh_3$ ligands of the first two complex molecules. These C–H···O and C–H···π interactions are extended throughout the entire lattice of **3**. The noncovalent interactions, observed in all three crystals, play a key role in the packing of the molecules in the crystals, and it may be relevant to note here that such interactions are of significant importance in molecular recognition processes as well as in crystal engineering.[11]

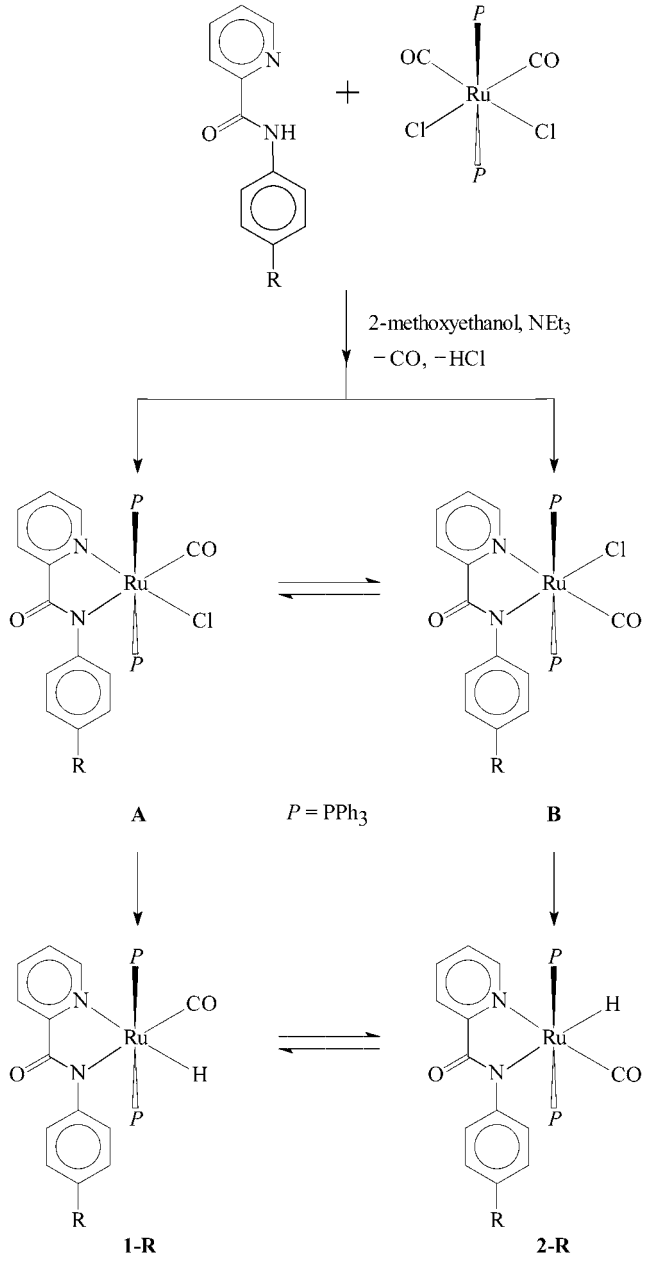


Scheme 1.

 © 2007 Wiley-VCH Verlag GmbH & Co. KGaA, Weinheim 

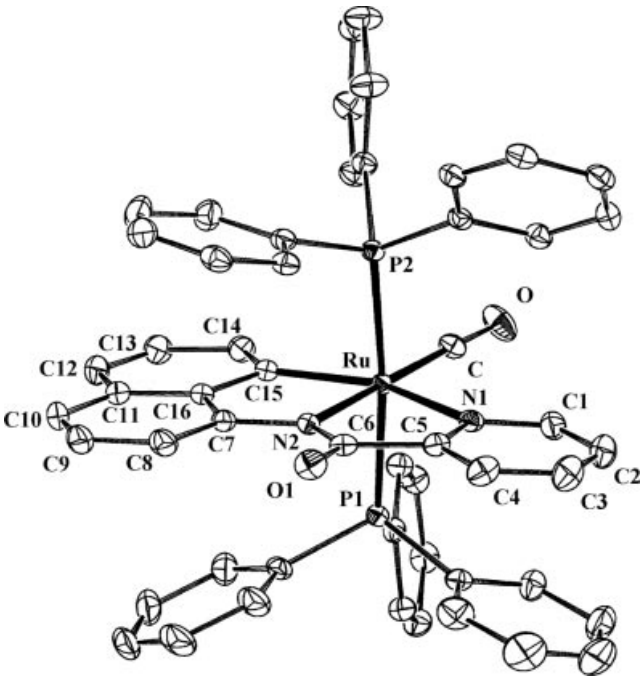


Figure 4. View of complex **3**.

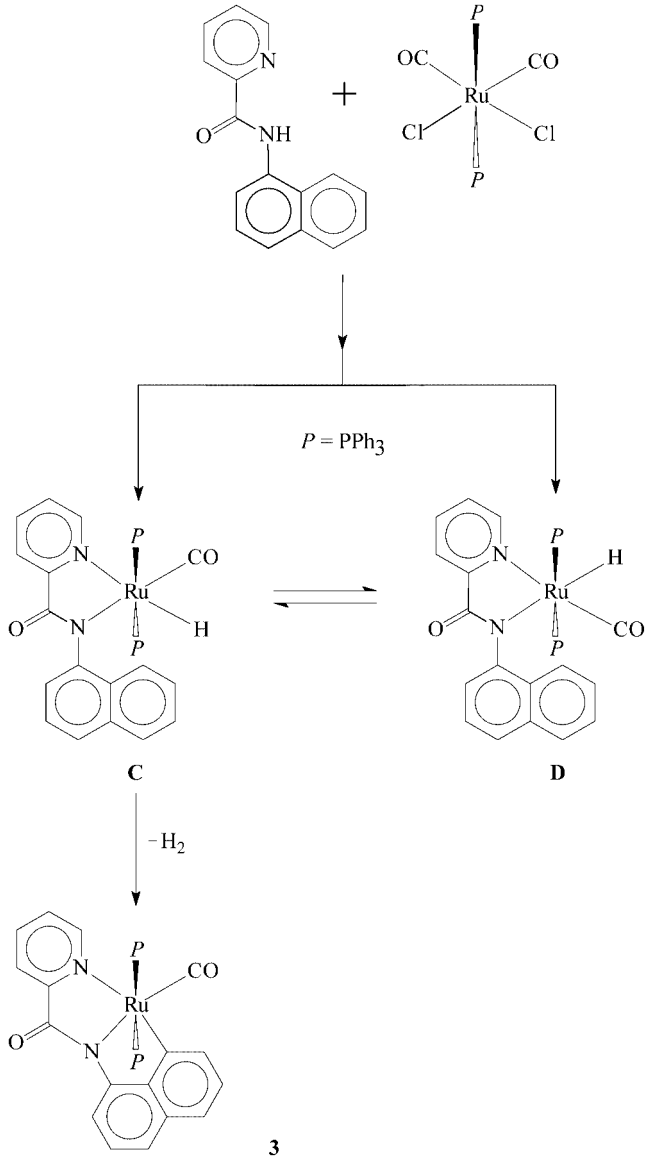


Scheme 2.

Probable sequences behind formation of the cyclometalated complex **3** are illustrated in Scheme 2. In the early stage of the synthetic reaction an equilibrium mixture of two stereoisomers (**C** and **D**) of a hydride intermediate (as shown in Scheme 1) are believed to be formed, in both of which ligand $\mathbf{L^2}$ is coordinated as a *N*,*N* donor. Isomer **C** of the intermediate then undergoes the C–H activation at the 8-position of the naphthyl ring affording the cyclometalated species **3** through elimination of molecular hydrogen.[12] As isomer **C** is irreversibly transformed into the cyclometalated species **3**, the equilibrium between the two isomers gradually shifts towards **C**, and thus only the cyclometalated species **3** is obtained as the sole product from this reaction and none of the two intermediates can be isolated.

Magnetic susceptibility measurements show that the **1-R**, **2-R**, and **3** complexes are diamagnetic, which corresponds to the +2 oxidation state of ruthenium (low-spin $d^6$, $S = 0$) in these complexes. $^1$H NMR spectra of the **1-R** complexes show broad signals within 7.1–7.7 ppm for the coordinated $PPh_3$ ligands. The hydride signal is observed as a distinct triplet, because of coupling with two magnetically equivalent phosphorus nuclei, near δ = –10.6 ppm. Most of the aromatic proton signals from the coordinated amide ligand are clearly observed in the expected region, while a few could not be detected because of their overlap with other signals in the same region. Signals for the methoxy and methyl groups in the **1-OCH$_3$** and **1-CH$_3$** complexes are observed respectively at $\delta$ = 3.67 and 2.11 ppm. In the $^1$H NMR spectra of the **2-R** complexes, the hydride signal (triplet) is observed at around δ = –12.1 ppm, and this significant shift in position, compared to the **1-R** complexes, has been useful as a diagnostic property in distinguishing this group of **2-R** complexes from their **1-R** isomers. Besides small shifts in the signal positions, the rest of the $^1$H NMR spectrum of each **2-R** complex is qualitatively similar to that of the corresponding **1-R** complex. It may be mentioned here that in $CDCl_3$ solution, each **1-R** (or **2-R**) complex is slowly and partially converted into the corresponding **2-R** (or **1-R**) isomer, which is easily recognized by the appearance of the characteristic hydride signal of the generated isomer. It may also be noted that conversion of **1-R** to **2-R** is relatively faster (takes about 6 d to reach equilibrium, where concentration ratio of **1-R** and **2-R** becomes approximately 2:1), while that of **2-R** to **1-R** is much slower (takes about 8 d to reach a concentration ratio of **1-R** and **2-R** of approximately 1:8). Except for the absence of the hydride signal and the presence of a few additional signals in the aromatic region, $^1$H NMR spectral features of complex **3** are similar to those of the **1-H** complex. $^{31}$P NMR spectra of all the **1-R** and **2-R** complexes show a single resonance

 © 2007 Wiley-VCH Verlag GmbH & Co. KGaA, Weinheim 

near 41.7 and 44.0 ppm respectively. In complex **3**, the $^{31}P$ signal is observed at $\delta$ = 31.42 ppm.

The infrared spectrum of each **1-R** complex shows many bands of different intensities in the 400–4000 $cm^{-1}$ region. Assignment of each individual band to a specific vibration has not been attempted. However, comparison with the spectra of the corresponding uncoordinated ligands shows that the N–H stretch, observed near 3140 $cm^{-1}$ in the uncoordinated ligands, is absent in the complexes. The amide C=O stretch, observed at around 1680 $cm^{-1}$ in the uncoordinated ligands, is also found to be shifted to around 1578 $cm^{-1}$ in the complexes. A strong band observed near 1900 $cm^{-1}$ in all the **1-R** complexes is due to the coordinated carbon monoxide, and three strong bands have been observed near 517, 692, and 746 $cm^{-1}$ in **1-R** complexes, indicating the presence of the coordinated $PPh_3$ ligands.[2m] Sharp bands are also observed near 1092, 1433, 1479, and 1557 $cm^{-1}$ in the **1-R** complexes, which are found to be absent in the spectrum of $[Ru(PPh_3)_2(CO)_2Cl_2]$, and hence these are attributed to the coordinated *N*-(aryl)picolinamide. Infrared spectra of the **2-R** and **3** complexes are similar to those of the **1-R** complexes. The $^1H$ NMR and IR spectroscopic data of the **1-R**, **2-R**, and **3** complexes are therefore consistent with their compositions.

The **1-R**, **2-R**, and **3** complexes are soluble in acetone, dichloromethane, chloroform, and so forth, producing bright yellow solutions. Electronic spectra of the complexes have been recorded in dichloromethane solution. All the complexes show several intense absorptions in the visible and ultraviolet regions (Table 2). The absorptions in the ultraviolet region are attributable to transitions within the ligand orbitals and those in the visible region are probably due to charge-transfer transitions. To have a better insight into the nature of the absorptions in the visible region, qualitative EHMO calculations have been performed[13] on computer-generated models of the complexes where phenyl rings of the triphenylphosphanes have been replaced by hydrogen. Partial MO diagrams of a selected **1-R** complex are shown in Figure 5 and those of a representative **2-R** and **3** complexes are deposited as supporting information (Figures S3 and S4). Compositions of selected molecular orbitals are given in Table S1 (supporting information). In the **1-R** complexes, the highest occupied molecular orbital (HOMO) and the next two filled orbitals (HOMO-1 and HOMO-2) have major contributions from the ruthenium $d_{xy}$, $d_{yz}$, and $d_{xz}$ orbitals.[14] These three occupied orbitals may therefore be regarded as the ruthenium $t_2$ orbitals. The lowest unoccupied molecular orbital (LUMO) has more than 90% contribution from the *N*-(aryl)picolinamide and is concentrated largely on the pyridine ring and the amido fragment. Among the next few vacant orbitals (LUMO+1, LUMO+2 etc.), LUMO+1 is primarily centered on the pyridine ring, while LUMO+2 is delocalized over both the pyridine ring and the pendent phenyl ring of the *N*-(aryl)picolinamide. The lowest energy absorption in the 392–420 nm region may therefore be assigned to the charge-transfer transition taking place from the highest filled ruthenium $t_2$ orbital (HOMO) to the vacant orbital delocalized over the *N*-(aryl)picolinamide (LUMO). The other intense absorptions in the visible region may be assigned to charge-transfer transitions from the ruthenium $t_2$ orbitals to the higher-energy vacant orbitals. The nature of the molecular orbitals in the **2-R** complexes is very similar to that in the **1-R** complexes, and the electronic spectral features of these two groups of complexes are also very similar. In complex **3**, however, the HOMO, HOMO-1, and HOMO-2 are found to have large contributions from the *N*-(naphthyl)picolinamide besides having significant contributions from the ruthenium $d_{xy}$, $d_{yz}$, and $d_{xz}$ orbitals. The LUMO of complex **3** is concentrated largely on the pyridine ring and the carbonamide functionality. The next two vacant orbitals (LUMO+1 and LUMO+2) are close in energy; LUMO+1 is primarily centered on the pyridine ring, while LUMO+2 is delocalized over both the naphthyl and pyridine ring of the *N*-(naphthyl)picolinamide. The absorption at 472 nm may therefore be assigned to a HOMO-to-LUMO charge-transfer transition and the other absorptions in the visible region to charge-transfer transitions from the filled orbitals to the higher-energy vacant orbitals.

Table 2. Electronic spectral and cyclic voltammetric data.

| | Electronic spectroscopic data[a] | Cyclic voltammetric data[b] | |
|---|---|---|---|
| | $\lambda_{max}$ [nm] ($\varepsilon$ [$M^{-1}cm^{-1}$]) | $E_{pa}$ [V] | $E_{pc}$ [V] |
| **1-$OCH_3$** | 230 (55300), 254[c] (32400), 348 (7800), 400 (3800) | 0.71, 1.29 | –1.19 |
| **1-$CH_3$** | 230 (34900), 254[c] (21600), 338 (5300), 396 (1800) | 0.77, 1.31 | –1.21 |
| **1-H** | 230 (35500), 254[c] (25300), 336 (6800), 392 (2500) | 0.80, 1.47 | –1.19 |
| **1-Cl** | 230 (32700), 256[c] (22800), 340 (7400), 394 (4100) | 0.83, 1.56 | –1.13 |
| **1-$NO_2$** | 230 (37800), 254[c] (25400), 322 (9400), 420 (1500) | 0.93, 1.69 | –1.12 |
| **2-$OCH_3$** | 230 (50300), 272[c] (19700), 354 (5600), 430 (2250) | 0.54, 1.26 | –1.05 |
| **2-$CH_3$** | 230 (95900), 272[c] (31250), 362 (7580), 432 (3000) | 0.55, 1.28 | –1.03 |
| **2-H** | 230 (47900), 274[c] (15100), 368 (3600), 424 (1700) | 0.60, 1.32 | –1.11 |
| **2-Cl** | 230 (36000), 274[c] (13480), 356 (3800), 440 (980) | 0.64, 1.35 | –1.10 |
| **2-$NO_2$** | 230 (15500), 278[c] (4800), 348 (3000), 448 (2600) | 0.69, 1.42 | –1.09 |
| **3** | 246 (28900), 348 (11800), 472 (2000) | 0.49, 1.34 | –1.02 |

[a] In dichloromethane. [b] Solvent: dichloromethane/acetonitrile, 1:9; supporting electrolyte, TBAP; reference electrode, SCE; $E_{pa}$ and $E_{pc}$ are anodic and cathodic peak potentials; scan rate, 50 $mV s^{-1}$. [c] Shoulder.

Electrochemical properties of the **1-R**, **2-R**, and **3** complexes have been studied by cyclic voltammetry in 1:9 dichloromethane/acetonitrile solution (0.1 M TBAP).[15] Each complex shows two anodic waves at positive potentials of the SCE reference electrode and a cathodic one at negative potential (Table 2). All the responses are irreversible in nature. In view of the composition of the HOMO, the first oxidation is assigned to $Ru^{II}$–$Ru^{III}$ oxidation. Simi-

 © 2007 Wiley-VCH Verlag GmbH & Co. KGaA, Weinheim 

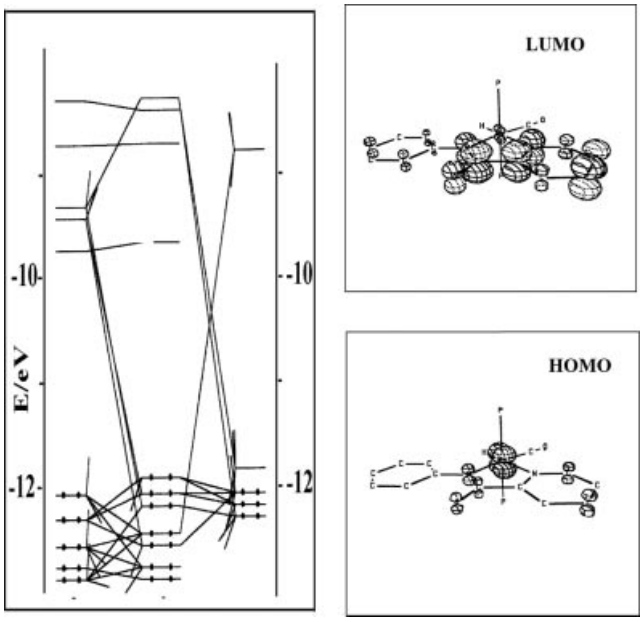


Figure 5. Partial molecular orbital diagram of the **1-H** complex.

larly based on composition of the LUMO, the reduction is assigned to reduction of the coordinated amide ligand. The second oxidation is attributed tentatively to oxidation of the coordinated amide ligand. Comparison of the potential of the $Ru^{II}$–$Ru^{III}$ couple in the **1-R** and **2-R** complexes shows that the bivalent state of ruthenium is much more stabilized in the former group of complexes, which may be attributed to the presence of carbonyl ligand *cis* to the pyridine nitrogen in the coordination sphere of ruthenium in the **1-R** complexes, favoring the back donation from the metal center to these two π-acidic ligands, rendering the ruthenium(II) state much more stable than the **2-R** complexes. In these **1-R** and **2-R** complexes, the potential of the $Ru^{II}$–$Ru^{III}$ oxidation has been observed to be sensitive to the nature of the substituent R in the *N*-(aryl)picolinamide. The potential ($E_{pa}$) increases with increasing electron-withdrawing character of the substituent R. The plots of $E_{pa}$ versus $\sigma$ [$\sigma$ = Hammett constant of R;[16] for $OCH_3$: –0.27, $CH_3$: –0.17, H: 0.00, Cl: 0.23, $NO_2$: 0.78] are linear for both the **1-R** and **2-R** complexes (see Figures S5 and S6 in the supporting information) with slopes ($\rho$) of 0.19 and 0.15 V ($\rho$ = reaction constant of this oxidation[17]) respectively. For both **1-R** and **2-R** complexes, the potential of the second oxidative response also shows linear correlation with the electron-withdrawing nature of substituent R (Figures S7 and S8, supporting information), with slopes ($\rho$) of 0.39 and 0.15 V, respectively. Potentials of the irreversible reductive response do not show any systematic variation with the nature of the substituent R.

## Conclusions

The present study shows that upon reaction with $[Ru(PPh_3)_2(CO)_2Cl_2]$ the *N*-(aryl)picolinamides (**$L^1$**) can bind to ruthenium as monoanionic *N*,*N*-donors by displacing a carbonyl and a chloride, as well as turning a Ru–Cl bond into a Ru–H bond. This study also demonstrates that the Ru–H bond can be utilized for inducing C–H activation of selective amides, such as *N*-(naphthyl)picolinamide. Utilization of the Ru–H bond for other useful reactions is currently under exploration.

## Experimental Section

**General Procedure:** Commercial ruthenium trichloride was purchased from Arora Matthey, Kolkata, India and was converted to $[Ru(PPh_3)_2(CO)_2Cl_2]$ by following a reported procedure.[18] The *N*-(aryl)picolinamides were prepared by condensing picolinic acid with *para*-substituted anilines or α-naphthylamine.[8a] Purification of dichloromethane and acetonitrile, and preparation of tetrabutylammonium perchlorate (TBAP) for electrochemical work were performed as reported in the literature.[19] All other chemicals and solvents were reagent grade commercial materials and were used as received. Microanalyses (C, H, N) were performed using a Heraeus Carlo Erba 1108 elemental analyzer. Magnetic susceptibilities were measured using a PAR 155 vibrating sample magnetometer fitted with a Walker scientific L75FBAL magnet. $^1$H NMR spectra were recorded in $CDCl_3$ solution with a Bruker Avance DPX 300 NMR spectrometer using TMS as the internal standard. IR spectra were obtained with a Shimadzu FTIR-8300 spectrometer with samples prepared as KBr pellets. Electronic spectra were recorded with a JASCO V-570 spectrophotometer. Electrochemical measurements were made using a CH Instruments model 600A electrochemical analyzer. A platinum disc working electrode, a platinum wire auxiliary electrode, and an aqueous saturated calomel reference electrode (SCE) were used in the cyclic voltammetry experiments. All electrochemical experiments were performed under dinitrogen. All electrochemical data were collected at 298 K and are uncorrected for junction potentials.

### Preparations of Complexes

The **1-R** and **2-R** complexes were obtained by following a general procedure. Specific details are given below for a particular pair of complexes.

**1-$OCH_3$ and 2-$OCH_3$:** *N*-(4-Methoxyphenyl)picolinamide (**$L^1$**, R = $OCH_3$) (30 mg, 0.13 mmol) was dissolved in warm 2-methoxyethanol (50 mL) and triethylamine (13 mg, 0.13 mmol) was added to it followed by $[Ru(PPh_3)_2(CO)_2Cl_2]$ (100 mg, 0.13 mmol). The mixture was refluxed for 24 h, whereby a yellow solution was obtained. Evaporation of this solution afforded a dark yellow solid, which was subjected to purification by thin layer chromatography on a silica plate. With 1:3 acetonitrile/benzene as the eluent, a distinct golden yellow band separated first followed by an orangish-yellow band, both of which were extracted separately with 1:3 dichloromethane/acetonitrile. Evaporation of these extracts respectively gave **1-$OCH_3$** as a crystalline golden yellow solid and **2-$OCH_3$** as a yellow crystalline solid.

**1-$OCH_3$:** Yield: 35 mg, 30%. $C_{50}H_{42}N_2O_3P_2Ru$ (881): calcd. C 68.10, H 4.76, N 3.17; found C 67.47, H 4.80, N 3.19. $^1$H NMR:[20] $\delta$ = –10.64 (t, $J$ = 19.5 Hz, 1 H); 3.67 ($OCH_3$); 6.20 (d, $J$ = 9.0 Hz, 2 H); 6.65 (t, $J$ = 5.7 Hz, 1 H); 6.84 (d, $J$ = 9.0 Hz, 2 H); 7.14–7.72 ($2PPh_3$+d)*; 7.92 (d, $J$ = 5.0 Hz, 1 H) ppm. $^{31}$P NMR: $\delta$ = 41.72 ppm. **1-$CH_3$:** Yield: 38 mg, 33%. $C_{50}H_{42}N_2O_2P_2Ru$ (865): calcd. C 69.36, H 4.85, N 3.23; found C 69.07, H 4.88, N 3.25. $^1$H NMR: $\delta$ = –10.59 (t, $J$ = 19.4 Hz, 1 H); 2.11 ($CH_3$); 6.41 (d, $J$ = 8.2 Hz, 2 H); 6.65 (t, $J$ = 6.2 Hz, 1 H); 6.73 (d, $J$ = 8.2 Hz, 2 H); 7.12–7.46 ($2PPh_3$); 7.69 (d, $J$ = 7.8 Hz, 1 H); 7.93 (d, $J$ = 5.0 Hz, 1 H) ppm.

 © 2007 Wiley-VCH Verlag GmbH & Co. KGaA, Weinheim 

$^{31}$P NMR: $\delta$ = 41.74 ppm. **1-H:** Yield: 34 mg, 30%. $C_{49}H_{40}N_2O_2P_2Ru$ (851): calcd. C 69.09, H 4.93, N 3.29; found C 68.67, H 4.92, N 3.26. $^1$H NMR: $\delta$ = –10.54 (t, $J$ = 19.4 Hz, 1 H); 6.60–6.68 (t + t + t, 3 H)*; 6.92 (d, $J$ = 6.1 Hz, 2 H); 7.13–7.49 (2PPh$_3$); 7.73 (d, $J$ = 7.8 Hz, 1 H); 7.92 (d, $J$ = 5.0 Hz, 1 H) ppm. $^{31}$P NMR: $\delta$ = 41.71 ppm. **1-Cl:** Yield: 38 mg, 32%. $C_{49}H_{39}ClN_2O_2P_2Ru$ (885.5): calcd. C 66.40, H 4.40, N 3.16; found C 66.07, H 4.46, N 3.14. $^1$H NMR: $\delta$ = –10.64 (t, $J$ = 19.4 Hz, 1 H); 6.54 (d, $J$ = 8.9 Hz, 2 H); 6.64 (t, $J$ = 6.1 Hz, 1 H); 6.87 (d, $J$ = 8.8 Hz, 2 H); 7.13–7.43 (2PPh$_3$); 7.731 (d, $J$ = 7.8 Hz, 1 H); 7.90 (d, $J$ = 5.0 Hz, 1 H) ppm. $^{31}$P NMR: $\delta$ = 41.72 ppm. **1-NO$_2$:** Yield: 40 mg, 34%. $C_{49}H_{39}N_3O_4P_2Ru$ (896): calcd. C 65.62, H 4.35, N 3.12; found C 65.30, H 4.30, N 3.14. $^1$H NMR: $\delta$ = –10.64 (t, $J$ = 19.4 Hz, 1 H); 6.72 (t, $J$ = 6.3 Hz, 1 H); 7.13–7.43 (2PPh$_3$); 7.48 (d, $J$ = 6.0 Hz, 2 H); 7.79 (d, $J$ = 7.8 Hz, 1 H), 7.95 (d, $J$ = 5.1 Hz, 1 H) ppm. $^{31}$P NMR: $\delta$ = 41.73 ppm.

**2-OCH$_3$:** Yield: 40 mg, 35%. $C_{50}H_{42}N_2O_3P_2Ru$ (881): calcd. C 68.10, H 4.76, N 3.17; found C 67.80, H 4.80, N 3.21. $^1$H NMR: $\delta$ = –12.16 (t, $J$ = 20.5 Hz, 1 H); 3.77 (OCH$_3$); 6.20 (t, $J$ = 6.4 Hz, 1 H); 6.46 (d, $J$ = 8.9 Hz, 2 H); 6.82 (d, $J$ = 8.9 Hz, 2 H); 7.10–7.40 (2PPh$_3$); 7.47 (d, $J$ = 5.3 Hz, 1 H); 7.62 (d, $J$ = 7.6 Hz, 1 H) ppm. $^{31}$P NMR: $\delta$ = 44.09 ppm. **2-CH$_3$:** Yield: 37 mg, 32%. $C_{50}H_{42}N_2O_2P_2Ru$ (865): calcd. C 69.36, H 4.85, N 3.23; found C 69.24, H 4.82, N 3.19. $^1$H NMR: $\delta$ = –12.05 (t, $J$ = 20.7 Hz, 1 H); 2.24 (CH$_3$); 6.21 (t, $J$ = 6.3 Hz, 1 H); 6.69 (d, $J$ = 8.1 Hz, 2 H); 6.78 (d, $J$ = 8.1 Hz, 2 H); 7.11–7.48 (2PPh$_3$); 7.48–7.70 (t + d + d, 3 H)* ppm. $^{31}$P NMR: $\delta$ = 44.04 ppm. **2-H:** Yield: 37 mg, 33%. $C_{49}H_{40}N_2O_2P_2Ru$ (851): calcd. C 69.09, H 4.93, N 3.29; found C 68.87, H 4.92, N 3.26. $^1$H NMR: $\delta$ = –12.09 (t, $J$ = 20.7 Hz, 1 H); 6.21 (t, $J$ = 6.2 Hz, 1 H); 6.85–6.89 (2d + 2t, 4 H)*; 7.11–7.48 (2PPh$_3$); 7.53–7.60 (t + d, 2 H)*; 7.69 (d, $J$ = 7.0 Hz, 1 H) ppm. $^{31}$P NMR: $\delta$ = 44.06 ppm. **2-Cl:** Yield: 40 mg, 34%. $C_{49}H_{39}ClN_2O_2P_2Ru$ (885.5): calcd. C 66.40, H 4.40, N 3.16; found C 66.17, H 4.35, N 3.12. $^1$H NMR: $\delta$ = –12.16 (t, $J$ = 20.5 Hz, 1 H); 6.20 (t, $J$ = 6.3 Hz, 1 H); 6.52–6.80 (d + d, 4 H)*; 7.11–7.63 (2PPh$_3$); 7.82 (d, $J$ = 5.1 Hz, 1 H) ppm. $^{31}$P NMR: $\delta$ = 44.10 ppm. **2-NO$_2$:** Yield: 40 mg, 34%. $C_{49}H_{39}N_3O_4P_2Ru$ (896): calcd. C 65.62, H 4.35, N 3.12; found C 65.38, H 4.31, N 3.11. $^1$H NMR: $\delta$ = –12.36 (t, $J$ = 20.1 Hz, 1 H); 6.24 (t, $J$ = 6.2 Hz, 1 H); 6.93 (d, $J$ = 9.0 Hz, 2 H); 7.11–7.36 (2PPh$_3$); 7.51 (d, $J$ = 8.1 Hz, 1 H); 7.66 (d, $J$ = 8.3 Hz, 1 H); 7.70 (d, $J$ = 9.3 Hz, 2 H) ppm. $^{31}$P NMR: $\delta$ = 44.14 ppm.

**3:** *N*-(1-Naphthyl)picolinamide (**L$^2$**) (32 mg, 0.13 mmol) was dissolved in warm 2-methoxyethanol (50 mL) and triethylamine (13 mg, 0.13 mmol) was added to it followed by [Ru(PPh$_3$)$_2$(CO)$_2$Cl$_2$] (100 mg, 0.13 mmol). The mixture was refluxed for 24 h, whereby a yellow solution was obtained. Evaporation of this solution afforded an orange solid, which was subjected to purification by thin layer chromatography on a silica plate. With 1:3 acetonitrile/benzene as the eluent, a distinct orange band separated, which was extracted with 1:3 dichloromethane/acetonitrile. Evaporation of this extract gave **3** as a crystalline orange solid. Yield: 84 mg, 70%. $C_{53}H_{40}N_2O_2P_2Ru$ (899): calcd. C 71.54, H 4.49, N 3.14; found C 72.23, H 4.46, N 3.11. $^1$H NMR: $\delta$ = 6.62 (t, $J$ = 6.2 Hz, 1 H); 6.76 (t, $J$ = 7.5 Hz, 1 H); 6.82–6.90 (t + 2d, 3 H)*, 6.99–7.15 (2PPh$_3$); 7.36 (t, $J$ = 7.8 Hz, 1 H); 7.48 (d, $J$ = 6.3 Hz, 1 H); 7.69 (d, $J$ = 7.9 Hz, 1 H), 8.05–8.07 (d + d, 2 H)* ppm. $^{31}$P NMR: $\delta$ = 31.42 ppm.

**X-ray Crystallography:** Single crystals of the **1-OCH$_3$** and **3** complexes were obtained by slow evaporation of acetonitrile solutions of the respective complexes. Single crystals of the **2-CH$_3$** complex were obtained by slow evaporation of a solution of the complex in a 1:1 mixture of methanol and dichloromethane. Selected crystal data and data collection parameters are given in Table 3. Data were collected on a Bruker CCD diffractometer using graphite-monochromated Mo-$K_\alpha$ radiation. X-ray data reduction, and structure solution and refinement were done using SHELXS-97 and SHELXL-97 programs.[21] The structures were solved by the direct methods.

CCDC-623582, -623583, and -623584 contain the supplementary crystallographic data for this paper. These data can be obtained free of charge from The Cambridge Crystallographic Data Centre via www.ccdc.cam.ac.uk/data_request/cif.

**Supporting Information** (see also the footnote on the first page of this article): Packing diagram showing hydrogen bonding in complexes **2-CH$_3$** (Figure S1) and **3** (Figure S2), partial molecular orbital diagrams of complexes **2-H** (Figure S3) and **3** (Figure S4), least-squares plots of $E_{pa}$ values of $Ru^{II}$–$Ru^{III}$ couple versus Ham-

Table 3. Crystallographic data for **1-OCH$_3$**, **2-CH$_3$** and **3**.

| | **1-OCH$_3$·2H$_2$O** | **2-CH$_3$·CH$_3$OH** | **3** |
|---|---|---|---|
| Empirical formula | $C_{50}H_{46}N_2O_5P_2Ru$ | $C_{51}H_{46}N_2O_3P_2Ru$ | $C_{53}H_{40}N_2O_2P_2Ru$ |
| Formula mass | 917.90 | 897.91 | 899.88 |
| Space group | triclinic, $P\bar{1}$ | monoclinic, $P2_1/c$ | monoclinic, $Cc$ |
| $a$ [Å] | 10.1885(10) | 19.958(3) | 11.6130(7) |
| $b$ [Å] | 13.7277(13) | 10.8273(18) | 22.0267(14) |
| $c$ [Å] | 15.0590(14) | 19.795(3) | 16.7471(11) |
| $\alpha$ [°] | 87.675(2) | 90 | 90 |
| $\beta$ [°] | 89.174(2) | 103.234(3) | 109.2660(10) |
| $\gamma$ [°] | 82.557(2) | 90 | 90 |
| $V$ [Å$^3$] | 2086.7(3) | 4164.1(12) | 4043.9(4) |
| $Z$ | 2 | 4 | 4 |
| $\lambda$ [Å] | 0.71073 | 0.71073 | 0.71073 |
| Crystal size [mm] | 0.66 × 0.45 × 0.15 | 0.44 × 0.35 × 0.15 | 0.17 × 0.36 × 0.67 |
| $T$ [K] | 293(2) | 293(2) | 103(2) |
| $\mu$ [mm$^{-1}$] | 0.505 | 0.501 | 0.514 |
| $R1$[a] | 0.0337 | 0.0372 | 0.0211 |
| $wR2$[b] | 0.0847 | 0.0880 | 0.0517 |
| Gof[c] | 1.029 | 1.022 | 1.039 |

[a] $R1 = \Sigma||F_o| - |F_c||/\Sigma|F_o|$. [b] $wR2 = [\Sigma\{w(F_o^2 - F_c^2)^2\}/\Sigma\{w(F_o^2)\}]^{1/2}$. [c] Gof = $\{\Sigma[w(F_o^2 - F_c^2)^2]/(M - N)\}^{1/2}$, where $M$ is the number of reflections and $N$ is the number of parameters refined.

 © 2007 Wiley-VCH Verlag GmbH & Co. KGaA, Weinheim 

mett substituent constant ($\sigma$) for the **1-R** and **2-R** complexes (Figure S5 and Figure S6), least-squares plots of $E_{pa}$ values of ligand-centered oxidation versus Hammett substituent constant ($\sigma$) for the **1-R** and **2-R** complexes (Figure S7 and Figure S8), composition of selected molecular orbitals for all the complexes (Table S1), and X-ray crystallographic data in CIF format.

## Acknowledgments

Financial assistance received from the Department of Science and Technology [Grant No. SR/S1/IC-15/2004] is gratefully acknowledged. S. N. thanks the Council of Scientific and Industrial Research, New Delhi, for his fellowship [Grant No. 9/96(401)2003-EMR-I].

[1] a) M. Turki, C. Daniel, *Coord. Chem. Rev.* **2001**, *216–217*, 31; b) V. Balzani, A. Juris, *Coord. Chem. Rev.* **2001**, *211*, 97; c) B.-Z. Shan, Q. Zhao, N. Goswami, D. M. Eichhom, D. P. Rillema, *Coord. Chem. Rev.* **2001**, *211*, 117; d) N. A. P. Kane-Maguire, J. F. Wheeler, *Coord. Chem. Rev.* **2001**, *211*, 145; e) L.-N. Ji, X.-H. Zou, J.-G. Liu, *Coord. Chem. Rev.* **2001**, *216–217*, 513; f) G. Simonneaux, P. Le Maux, *Coord. Chem. Rev.* **2002**, *228*, 43; g) H. Yersin, C. Kratzer, *Coord. Chem. Rev.* **2002**, *229*, 75; h) J. F. Endicott, H. B. Schlegel, M. J. Uddin, D. S. Seniveratne, *Coord. Chem. Rev.* **2002**, *229*, 95; i) S. I. Gorelsky, A. B. P. Lever, M. Ebadi, *Coord. Chem. Rev.* **2002**, *230*, 97; j) F. Hartl, M. P. Aarnts, H. A. Nieuwenhuis, J. van Slageren, *Coord. Chem. Rev.* **2002**, *230*, 106; k) C.-M. Che, J.-S. Huang, *Coord. Chem. Rev.* **2002**, *231*, 151; l) M. J. Clarke, *Coord. Chem. Rev.* **2002**, *232*, 69; m) E. Tfouni, M. Krieger, B. R. McGarvey, D. W. Franco, *Coord. Chem. Rev.* **2003**, *236*, 57; n) B. Serli, E. Zangrando, T. Gianferrara, L. Yellowless, E. Alessio, *Coord. Chem. Rev.* **2003**, *245*, 73; o) I. Ando, *Coord. Chem. Rev.* **2004**, *248*, 185; p) M. J. Clarke, *Coord. Chem. Rev.* **2003**, *236*, 209; q) M. A. S. Aquino, *Coord. Chem. Rev.* **2004**, *248*, 1025; r) R. F. Winter, S. Záli, *Coord. Chem. Rev.* **2004**, *248*, 1565; s) S. Rigaut, D. Touchard, P. H. Dixneuf, *Coord. Chem. Rev.* **2004**, *248*, 1585; t) M. K. Nazeeruddin, S. M. Zakeeruddin, J.-J. Lagref, P. Liska, P. Comte, C. Barolo, G. Viscardi, K. Schenk, M. Graetzel, *Coord. Chem. Rev.* **2004**, *248*, 1317; u) L. Spiccia, G. B. Deacon, C. M. Kepert, *Coord. Chem. Rev.* **2004**, *248*, 1329; v) Y. Saito, T. Azechi, T. Kitamura, Y. Hasegawa, Y. Wada, S. Yanagida, *Coord. Chem. Rev.* **2004**, *248*, 1469; w) Md. K. Nazeeruddin, C. Klein, P. Liska, M. Grätzel, *Coord. Chem. Rev.* **2005**, *249*, 1460.

[2] a) F. Basuli, S. M. Peng, S. Bhattacharya, *Inorg. Chem.* **1997**, *36*, 5645; b) F. Basuli, M. Ruf, C. G. Pierpont, S. Bhattacharya, *Inorg. Chem.* **1998**, *37*, 6113; c) A. K. Das, A. Rueda, L. R. Falvello, S. M. Peng, S. Bhattacharya, *Inorg. Chem.* **1999**, *38*, 4365; d) A. K. Das, S. M. Peng, S. Bhattacharya, *J. Chem. Soc., Dalton Trans.* **2000**, 181; e) F. Basuli, S. M. Peng, S. Bhattacharya, *Inorg. Chem.* **2000**, *39*, 1120; f) F. Basuli, S. M. Peng, S. Bhattacharya, *Inorg. Chem.* **2001**, *40*, 1126; g) I. Pal, F. Basuli, T. C. W. Mak, S. Bhattacharya, *Angew. Chem. Int. Ed.* **2001**, *40*, 2923; h) K. Majumder, R. J. Butcher, S. Bhattacharya, *Inorg. Chem.* **2002**, *41*, 4605; i) R. Acharyya, S. M. Peng, G. H. Lee, S. Bhattacharya, *Inorg. Chem.* **2003**, *42*, 7378; j) A. Das, S. M. Peng, G. H. Lee, S. Bhattacharya, *New. J. Chem.* **2004**, *28*, 712; k) S. Nag, P. Gupta, R. J. Butcher, S. Bhattacharya, *Inorg. Chem.* **2004**, *43*, 4814; l) P. K. Sinha, L. R. Falvello, S. Bhattacharya, *Indian J. Chem.* **2004**, *43A*, 1846; m) P. Gupta, S. Dutta, F. Basuli, S. M. Peng, G.-H. Lee, S. Bhattacharya, *Inorg. Chem.* **2006**, *45*, 460.

[3] a) P. Ford, D. E. P. Rudd, R. G. Gaunder, H. Taube, *J. Am. Chem. Soc.* **1968**, *90*, 1187; b) A. W. Zanella, P. C. Ford, *Inorg. Chem.* **1975**, *14*, 42; c) T. Matsubara, P. C. Ford, *Inorg. Chem.* **1976**, *15*, 1107; d) Y. Ilan, H. Taube, *Inorg. Chem.* **1983**, *22*, 1655; e) Y. Ilan, M. Kapon, *Inorg. Chem.* **1986**, *25*, 2350; f) H. Y. Huang, W. J. Chen, C. C. Yang, A. Yeh, *Inorg. Chem.* **1991**, *30*, 1862; g) M. H. Chou, C. Creutz, N. Sutin, *Inorg. Chem.* **1992**, *31*, 2318; h) M. H. Chou, B. S. Brunschwig, C. Creutz, N. Sutin, A. Yeh, R. C. Chang, C.-T. Lin, *Inorg. Chem.* **1992**, *31*, 5347; i) M. H. Chou, D. J. Szalda, C. Creutz, N. Sutin, *Inorg. Chem.* **1994**, *33*, 1674; j) S. M. Redmore, C. D. F. Rickard, S. J. Webb, L. J. Wright, *Inorg. Chem.* **1997**, *36*, 4743.

[4] B. Albert, D. Bray, J. Lewis, M. Raff, K. Roberts, J. D. Watson, *Molecular Biology of the Cell*, 3rd ed., Garland Publishing, New York, **1994**, ch. 3.

[5] a) H. Sigel, C. F. Naumann, B. Prijs, D. B. McCormick, M. C. Falk, *Inorg. Chem.* **1977**, *16*, 790; b) H. Sigel, *Inorg. Chem.* **1975**, *14*, 1535; c) M. F. El-Shazly, A. El-Dissowky, T. Salem, M. Osman, *Inorg. Chim. Acta* **1980**, *40*, 1; d) D. W. Margerum, *Pure Appl. Chem.* **1983**, *55*, 23; e) A. S. Borovik, T. M. Dewey, K. N. Raymond, *Inorg. Chem.* **1993**, *32*, 413; f) T. J. Collins, *Acc. Chem. Res.* **1994**, *27*, 279; g) M. J. Bartos, S. W. Gordon-Wylie, B. G. Fox, L. J. Wright, S. T. Weintraub, K. E. Kauffmann, E. Münck, K. L. Koskta, E. S. Uffelman, C. E. F. Rickard, K. R. Noon, T. J. Collins, *Coord. Chem. Rev.* **1998**, *174*, 361; h) A. White, X. Ding, J. C. vanderSpek, J. R. Murphy, D. Ringe, *Nature* **1998**, *394*, 502; i) E. Pohl, R. K. Holmes, W. G. J. Hol, *J. Mol. Biol.* **1999**, *292*, 653; j) B. M. Trost, C. B. Lee, *J. Am. Chem. Soc.* **2001**, *123*, 3671; k) M. D. Feese, B. P. Ingason, J. Goranson-Siekierke, R. K. Holmes, W. G. J. Hol, *J. Biol. Chem.* **2001**, *276*, 5959; l) T. J. Collins, *Acc. Chem. Res.* **2002**, *35*, 782; m) B. M. Trost, K. Dogra, I. Hachiya, T. Emura, D. L. Hughes, S. Krska, R. A. Reamer, M. Palucki, N. Yasuda, P. J. Reider, *Angew. Chem. Int. Ed.* **2002**, *41*, 1929; n) B. M. Trost, M. Crawley, *J. Am. Chem. Soc.* **2002**, *124*, 9328.

[6] T. Kojima, K. Hayashi, Y. Matsuda, *Inorg. Chem.* **2004**, *43*, 6793.

[7] a) H. Sigel, R. B. Martin, *Chem. Rev.* **1982**, *82*, 385; b) H. E. Bryndza, W. Tam, *Chem. Rev.* **1988**, *88*, 1163; c) K. Severin, R. Bergs, W. Beck, *Angew. Chem. Int. Ed.* **1998**, *37*, 1634; d) J. R. Fulton, A. W. Holland, D. J. Fox, R. G. Bergman, *Acc. Chem. Res.* **2002**, *35*, 44.

[8] a) S. Dutta, S. Pal, P. K. Bhattacharya, *Polyhedron* **1999**, *18*, 2157; b) S. Dutta, P. K. Bhattacharya, E. Horn, E. R. T. Tiekink, *Polyhedron* **2001**, *20*, 1815; c) S. Dutta, P. K. Bhattacharya, E. R. T. Tiekink, *Polyhedron* **2001**, *20*, 2027; d) A. K. Singh, V. Balamurugan, R. Mukherjee, *Inorg. Chem.* **2003**, *42*, 6497.

[9] a) F. Basuli, A. K. Das, G. Mostafa, S. M. Peng, S. Bhattacharya, *Polyhedron* **2000**, *19*, 1663; b) M. Menon, A. Pramanik, S. Chattopadhyay, N. Bag, A. Chakravorty, *Inorg. Chem.* **1995**, *34*, 1361; c) M. C. Barral, R. J. Aparicio, E. C. Royer, M. J. Saucedo, F. A. Urbanos, E. G. Puebla, C. R. Valero, *J. Chem. Soc., Dalton Trans.* **1991**, 1609.

[10] a) C. S. Yi, S. Y. Yun, I. A. Guzei, *Organometallics* **2004**, *23*, 5392; b) T. Li, R. Churlaud, A. J. Lough, K. Abdur-Rashid, R. H. Morris, *Organometallics* **2004**, *23*, 6239; c) R. Çelenligil-Çetin, L. A. Watson, C. Guo, B. M. Foxman, O. V. Ozerov, *Organometallics* **2005**, *24*, 186.

[11] a) S. K. Burley, G. A. Petsko, *Science* **1985**, *229*, 23; b) H. C. Weiss, D. Blaser, R. Boese, B. M. Doughan, M. M. Haley, *Chem. Commun.* **1997**, 1703; c) N. N. L. Madhavi, A. K. Katz, H. L. Carrell, A. Nangia, G. R. Desiraju, *Chem. Commun.* **1997**, 1953; d) S. K. Burley, G. A. Petsko, *Adv. Protein Chem.* **1988**, *39*, 125; e) M. Nishio, M. Hirota, Y. Umezawa, *The CH···π Interactions (Evidence, Nature and Consequences)*, Wiley-VCH, New York, **1998**; f) Y. Umezawa, S. Tsuboyama, K. Honda, J. Uzawa, M. Nishio, *Bull. Chem. Soc. Jpn.* **1998**, *71*, 1207; g) G. R. Desiraju, T. Steiner, *The Weak Hydrogen Bond (IUCr Monograph on Crystallography 9)*, Oxford Science Pub., USA, **1999**; h) M. J. Hannon, C. L. Painting, N. W. Alcock, *Chem. Commun.* **1999**, 2023; i) B. J. Mcnelis, L. C. Nathan, C. J. Clark, *J. Chem. Soc., Dalton Trans.* **1999**, 1831; j) K. Biradha, C. Seward, M. J. Zaworotko, *Angew. Chem. Int. Ed.* **1999**, *38*, 492; k) M. J. Calhorda, *Chem. Commun.* **2000**, 801; l) C. Janiak, S. Temizdemir, S. Dechert, *Inorg. Chem. Com-*

 © 2007 Wiley-VCH Verlag GmbH & Co. KGaA, Weinheim 

*mun.* **2000**, *3*, 271; m) C. Janiak, S. Temizdemir, S. Dechert, W. Deck, F. Girgsdies, J. Heinze, M. J. Kolm, T. G. Scarmann, O. M. Zipffel, *Eur. J. Inorg. Chem.* **2000**, 1229.
[12] The evolved hydrogen could not be detected experimentally.
[13] a) C. Mealli, D. M. Proserpio, *CACAO* Version 4.0, Italy, **1994**; b) C. Mealli, D. M. Proserpio, *J. Chem. Educ.* **1990**, *67*, 399.
[14] The HOMO of the **1-OCH$_3$** complex has little less contribution from ruthenium.
[15] A little dichloromethane was necessary to take the complex into solution. Addition of large excess of acetonitrile was necessary to record the redox responses in proper shape.
[16] L. P. Hammett, *Physical Organic Chemistry*, 2nd ed., McGraw Hill, New York, **1970**.
[17] R. N. Mukherjee, O. A. Rajan, A. Chakravorty, *Inorg. Chem.* **1982**, *21*, 785.
[18] N. Ahmad, S. D. Robinson, M. F. Uttley, *J. Chem. Soc., Dalton Trans.* **1972**, 843.
[19] a) D. T. Sawyer, J. L. Roberts Jr, *Experimental Electrochemistry for Chemists*, Wiley, New York, **1974**, pp. 167–215; b) M. Walter, L. Ramaley, *Anal. Chem.* **1973**, *45*, 165.
[20] Chemical shifts are given in ppm and multiplicity of the signals along with the associated coupling constants (*J* in Hz) are given in parentheses. Overlapping signals are marked with an asterisk.
[21] G. M. Sheldrick, *SHELXS-97* and *SHELXL-97*, Fortran programs for crystal structure solution and refinement, University of Göttingen, Göttingen, Germany, **1997**.

Received: October 13, 2006
Published Online: February 14, 2007

 © 2007 Wiley-VCH Verlag GmbH & Co. KGaA, Weinheim 